Kinetics of the Removal of OH($v = 1$) and OD($v = 1$) by HNO_3 and DNO_3 from 253 to 383 K

David C. McCabe,[†,‡,§] Steven S. Brown,[†,§] Mary K. Gilles,[†,§,||] Ranajit K. Talukdar,[†,§] Ian W. M. Smith,[⊥] and A. R. Ravishankara*[,†,‡,§]

NOAA Aeronomy Laboratory, 325 Broadway R/AL2, Boulder, Colorado 80305, Department of Chemistry and Biochemistry, University of Colorado, Boulder, Colorado 80309, Cooperative Institute for Research in Environmental Science, University of Colorado, Boulder, Colorado 80309, and School of Chemical Sciences, University of Birmingham, Edgbaston, Birmingham BI5 2TT, United Kingdom

Received: March 12, 2003; In Final Form: July 10, 2003

We have measured the rate coefficients for the removal of OH($v = 1$) and OD($v = 1$) by HNO_3 and DNO_3 as a function of temperature from 253 to 383 K. OH($v = 1$) and OD($v = 1$) were produced by photolysis of HNO_3/DNO_3 at 248 nm; laser-induced fluorescence was used to monitor the kinetics of the vibrationally excited radicals. The measured rate coefficients at 295 K range from 2.5×10^{-11} cm^3 molecule^{-1} s^{-1} for the removal of OH($v = 1$) by HNO_3 to 6×10^{-12} cm^3 molecule^{-1} s^{-1} for the removal of OH($v = 1$) by DNO_3; the rate coefficients for the like-isotope processes [removal of OH($v = 1$) by HNO_3 and removal of OD($v = 1$) by DNO_3] are 2−4 times higher than the rate coefficients for the unlike-isotope processes. All four rate coefficients show negative temperature dependences that are too strong to be attributable only to long-range interactions between the reactants. Expressed as negative activation energies, the temperature dependences yield values of E_a/R from −520 to −750 K. We suggest that the removal of the vibrationally excited radicals occurs via formation of the hydrogen-bonded, cyclic OH·HNO_3 reaction complex (or the appropriate isotopomer of the complex) invoked to explain the unusual kinetics of the reaction of ground-state OH with nitric acid. We postulate that dissociation of the reaction complex to regenerate nitric acid and vibrationally excited OH or OD competes with intramolecular vibrational redistribution of the OH/OD vibrational excitation energy within the reaction complex, leading to the observed negative temperature dependence. We attribute the higher rate coefficients of the like-isotope processes (relative to the unlike-isotope processes) to faster, resonant, intramolecular vibrational energy redistribution within the reaction complexes containing the same isotopes. Additionally, we estimate the yields of OH($v = 1$) to be ∼1% and OH($v = 2$) to be ∼0.4% of that of OH($v = 0$) from the photolysis of HNO_3 at 248 nm.

Introduction

The reaction of OH with nitric acid, reaction 1

$$OH + HNO_3 \rightarrow H_2O + NO_3 \qquad (1)$$

involves both HO_X ($HO_X \equiv OH + HO_2$) and NO_X ($NO_X \equiv NO + NO_2 + NO_3$) species and plays two important roles in the atmosphere. It is a sink for HO_X, and it converts HNO_3, a relatively unreactive reservoir for odd-nitrogen species, into NO_X. Therefore, reaction 1 affects the concentration of HO_X and the fraction of nitrogen oxides in the form of NO_X (i.e., the ratio of NO_X to NO_Y). The concentration of HO_X and the fraction of nitrogen oxides in the form of NO_X strongly affect the ozone concentration in the lower stratosphere and in the upper troposphere.

The kinetics of reaction 1 are unusual in several ways. Previous work has shown that the rate coefficient for this reaction, k_1, is pressure dependent at temperatures below ∼325 K, increases with decreasing temperature below ∼300 K, and is strongly affected by isotopic substitution of deuterium for the hydrogen in the nitric acid.[1,2]

Reaction 1 is thought to proceed via formation of a hydrogen-bonded OH·HNO_3 complex containing a six-membered ring, shown in Figure 1.[3] Previous work from this laboratory has shown that the observed kinetics of reaction 1 are compatible with a mechanism (also shown in Figure 1) involving this OH·HNO_3 complex.[2] Two groups have reported investigations of the OH·HNO_3 complex with ab initio methods,[4,5] showing that it is stable with respect to unbound OH and HNO_3 by ∼5−8 kcal mol^{-1}.

The species OH·HNO_3* shown in Figure 1 represents the nascent reactive complex OH·HNO_3 that has *not* been collisionally deactivated. It is difficult to determine rate coefficients for the association of reactants to form nascent reactive complexes, such as the rate coefficient k_a for the formation of the OH·HNO_3* complex from OH and HNO_3. This is particularly true if high-pressure data are unavailable. Smith and coworkers have proposed that one can estimate this type of rate coefficient (the high-pressure limit in the case of an association

* To whom correspondence should be addressed. E-mail: ravi@al.noaa.gov.
† NOAA Aeronomy Laboratory.
‡ Department of Chemistry and Biochemistry, University of Colorado.
§ CIRES, University of Colorado.
|| Current address: Chemical Sciences Division, Lawrence Berkeley National Laboratory, MS 6R2100, 1 Cyclotron Rd., Berkeley, California, 94720.
⊥ University of Birmingham.

10.1021/jp0346413 CCC: $25.00
Published on Web 09/06/2003

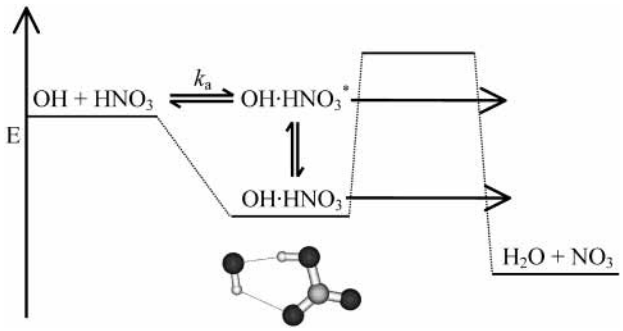

Figure 1. Mechanism for reaction 1 invoked by Brown et al.[2] to explain the observed kinetics of reaction 1. The mechanism involves formation of the $OH{\cdot}HNO_3$ complex, which subsequently reacts to form H_2O and NO_3.

reaction) by measuring the rate coefficient for the removal of one reactant that is excited with one quanta of vibrational excitation by the second reactant.[6−8] This approach assumes that the vibrational excitation is only removed by a mechanism involving the formation of the reaction complex; that the vibrational excitation does not affect the rate coefficient for formation of the complex; and that, if the reaction complex dissociates to re-form the reactants, the reactant that was originally vibrationally excited will be re-formed essentially only in the vibrational ground state.

To further investigate the mechanism of the reaction of OH with HNO_3, we have measured the rate coefficients for the removal of $OH(v = 1)$ and $OD(v = 1)$ by HNO_3 and DNO_3 as a function of temperature from 253 to 383 K

$$OH(v = 1) + HNO_3 \rightarrow \text{loss of } OH(v = 1) \qquad (2)$$

$$OH(v = 1) + DNO_3 \rightarrow \text{loss of } OH(v = 1) \qquad (3)$$

$$OD(v = 1) + HNO_3 \rightarrow \text{loss of } OD(v = 1) \qquad (4)$$

$$OD(v = 1) + DNO_3 \rightarrow \text{loss of } OD(v = 1) \qquad (5)$$

These rate coefficients should be approximately equal to k_a. Measuring the various isotopomeric combinations allows for the investigation of the effect of vibrational resonance between the reactants on these rate coefficients.

Use of rate coefficients for the loss of vibrationally excited reactants as an estimate of the rate coefficient for formation of a reactive complex has primarily been used to estimate k^∞, the rate coefficient for an association reaction between two radicals in the limit of high pressure.[6] In these cases, a covalent bond is formed between the two reactants, with bond energies greater than roughly 40 kcal mol^{-1}. When the $OH{\cdot}HNO_3$ complex forms, the bonds formed are hydrogen bonds, which are weaker ($OH{\cdot}HNO_3$ is bound by 5−8 kcal mol^{-1} [4,5]). In this paper, we also discuss whether the rate coefficients for reactions 2−5 are equivalent to k_a, given the differences between reaction 1 and typical association reactions. Last, we report measurements of the yields of $OH(v = 1)$ and $(v = 2)$, relative to the yield of $OH(v = 0)$, from the photolysis of HNO_3 at 248 nm.

Experimental Section

Rate coefficients k_2-k_5 were measured using pulsed laser photolysis of HNO_3 or DNO_3 to produce $OH(v = 1)$ or $OD(v = 1)$ and pulsed laser-induced fluorescence (LIF) detection of $OH(v = 1)$ or $OD(v = 1)$ in a slowly flowing mixture of HNO_3 and/or DNO_3 in He. The apparatus used to measure these rate coefficients has been used many times previously in our laboratory to measure rate coefficients for the reactions of ground-state OH and OD and is described in detail elsewhere.[9] This description focuses on the modifications to the previously described system that were required to study the kinetics of $OH(v = 1)$ and $OD(v = 1)$.

HNO_3 and DNO_3 were used as the photolytic precursors of $OH(v = 1)$ and $OD(v = 1)$. A mixture of HNO_3 and/or DNO_3 in He (both isotopomers were required for measurements of k_3 and k_4) was flowed at a linear flow velocity of ~10 cm s^{-1} through a jacketed, temperature-controlled glass cell. The total pressure in the reaction cell was approximately 30 Torr, consisting mostly of He. The 248-nm output of a KrF excimer laser was then passed through the cell (up to 60 mJ per pulse, beam size of ~1.5 cm^2) in a direction perpendicular to the gas flow to photolyze a fraction (≤0.1%) of the HNO_3 (DNO_3). A small fraction of the OH (OD) produced by photolysis is vibrationally excited.

This vibrationally excited $OH(v = 1)$ or $OD(v = 1)$ was monitored via laser-induced fluorescence. The second harmonic of a tunable dye laser pumped by the second harmonic of a pulsed Nd:YAG laser (532 nm) was passed through the reaction cell, perpendicular to both the gas flow and the photolysis laser. This probe laser excited the $Q_1(1)$ line of the $A^2\Sigma^+(v' = 0) \leftarrow X^2\Pi(v'' = 1)$ band (λ_{air} = 345.85 nm for OH,[10] 334.18 nm for OD[11]); fluorescence in the $A^2\Sigma^+(v' = 0) \rightarrow X^2\Pi(v'' = 0)$ band at ~308 nm was detected with a photomultiplier tube (PMT). The fluorescence passed through a band-pass filter (peak transmission at 307.5 nm, fwhm = 10 nm) between the reaction region (where the photolysis and probe laser beams intersect) and the PMT; this band-pass filter rejected scattered light from the lasers. Temporal profiles of $OH(v = 1)$ or $OD(v = 1)$ were generated by varying the delay time between the photolysis and probe lasers.

The yield of $OH(v = 1)$ from the 248-nm photolysis of HNO_3, relative to the yield of $OH(v = 0)$, was estimated by comparing the LIF signals (back-extrapolated to zero delay between the photolysis and probe lasers) from exciting the $Q_1(1)$ lines of the $A^2\Sigma^+(v' = 0) \leftarrow X^2\Pi(v'' = 1)$ band (λ_{air} = 345.85 nm) and the $A^2\Sigma^+(v' = 0) \leftarrow X^2\Pi(v'' = 0)$ band (λ_{air} = 307.84 nm).[10] The signals were recorded in back-to-back measurements, with the concentration of HNO_3 held constant.

The concentration of HNO_3 and/or DNO_3 was several orders of magnitude larger than the concentration of $OH(v = 1)$ or $OD(v = 1)$; therefore, the removal rate of the vibrationally excited radicals was pseudo-first-order in their concentration. However, the temporal profiles of $OH/OD(v = 1)$ were not single exponential because of the formation of $OH/OD(v > 1)$ in the 248-nm photolysis of HNO_3/DNO_3. [Photolysis of HNO_3 by 248-nm radiation to produce OH and NO_2 is exothermic by ~65 kcal mol^{-1}, so production of OH in vibrational states up to $(v = 7)$ is thermodynamically allowed.] The formation of $OH(v > 1)$ was confirmed by the detection of the LIF signal of $OH(v = 2)$ at the $Q_1(1)$ line of the $A^2\Sigma^+(v' = 1) \leftarrow X^2\Pi(v'' = 2)$ band (λ_{air} = 350.90 nm).[10] This signal was weak, but its temporal behavior appeared to be single-exponential, indicating that 248-nm photolysis of HNO_3 produces little $OH(v > 2)$ and, if any $OH(v > 2)$ is formed, it has a negligible influence on the measured temporal profiles. Thus, for reaction 2, where $OH(v = 1)$ is monitored with HNO_3 present, the temporal behavior of $OH(v = 1)$ is governed by three reactions, assuming that

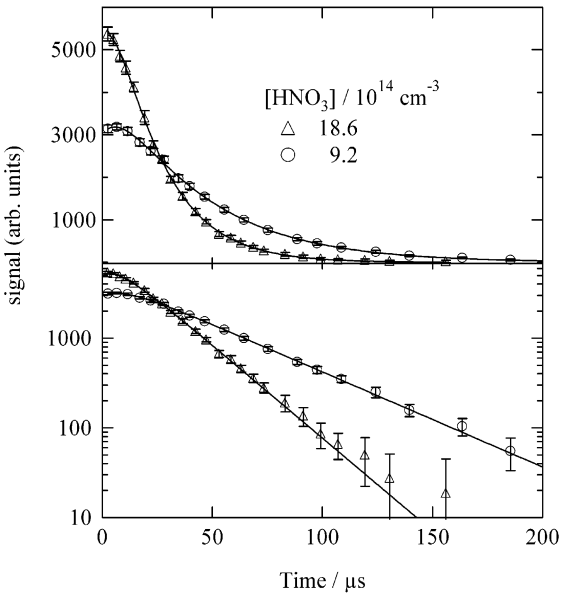

Figure 2. Temporal profiles of OH($v = 1$) at two nitric acid concentrations on linear (top panel) and logarithmic (bottom panel) scales, showing the non-single-exponential behavior of the signal at early times, due to reaction 6a. Fits to eq I are also shown.

vibrational relaxation by the He bath gas is negligible

$$\mathrm{OH}(v=2) + \mathrm{HNO_3} \rightarrow \mathrm{OH}(v=1) + \mathrm{HNO_3} \quad (6a)$$

$$\rightarrow \text{loss of OH}(v=2) \text{ not producing OH}(v=1) \quad (6b)$$

$$\mathrm{OH}(v=1) + \mathrm{HNO_3} \rightarrow \text{loss of OH}(v=1) \quad (2)$$

Using the pseudo-first-order rate coefficients $k_{6a}' \equiv k_{6a}[\mathrm{HNO_3}]$, $k_{6b}' \equiv k_{6b}[\mathrm{HNO_3}]$, $k_6' \equiv k_{6a}' + k_{6b}'$, and $k_2' \equiv k_2[\mathrm{HNO_3}]$, the concentration of OH($v = 1$) at time t is given by

$$[\mathrm{OH}(v=1)]_t = [\mathrm{OH}(v=1)]_0 \exp(-k_2't) + \frac{k_{6a}'[\mathrm{OH}(v=2)]_0}{k_2' - k_6'}[\exp(-k_6't) - \exp(-k_2't)] \quad \text{(I)}$$

where $[\mathrm{OH}(v = 1)]_0$, etc., are the concentrations of those reactants immediately after photolysis. The measured temporal profiles were fit to this form, with the assumption that $k_{6a}' = k_6'$. We made this assumption because k_{6a}' and $[\mathrm{OH}(v = 2)]_0$ are not independent variables in eq I; this assumption does not affect the measured values of k_2-k_5. The temporal profiles were fit well by eq I, indicating that, if OH($v > 2$) is formed, its concentration is not large enough to influence our measured values of k_2-k_5. It is possible that reaction 6b is significant, so that $k_{6a}' < k_6'$. Therefore, the fitted values of $[\mathrm{OH}(v = 2)]_0$ are lower limits. Figure 2 shows representative temporal profiles of OH($v = 1$) at two concentrations of $\mathrm{HNO_3}$, on linear and logarithmic scales. The biexponential nature of these temporal profiles is apparent in this figure.

It must be noted that, with biexponential temporal profiles such as those shown in Figure 2, the rate coefficients k_2' and k_6' cannot be independently assigned as the larger of the two will always govern the rise of the signal and the smaller of the two will always govern the decay of the signal, regardless of whether the faster reaction produces or consumes the monitored species. In this system, we assign the rise to k_6' because vibrational quenching is expected to be more rapid for higher vibrational levels. This assignment was confirmed by the temporal behavior of the OH($v = 2$) signal detected via excitation at 350.90 nm. Back-to-back temporal profiles of OH($v = 1$) and OH($v = 2$) were recorded, with the concentration of $\mathrm{HNO_3}$ held constant. The fitted rate coefficient for the rise in the temporal profile of OH($v = 1$) had a large uncertainty, but it was consistent with the first-order rate coefficient for the loss of OH($v = 2$). The OH($v = 2$) signal at 350.90 nm was also compared to the OH($v = 1$) signal at 345.85 nm to estimate the relative photolysis yields of these two states. However, this measurement is quite rough, because the two bands access different vibrational states of the electronically excited OH($A^2\Sigma^+$) species and the detection efficiency of our system is not the same for these different states.

Accurate LIF measurements at short reaction times ($<2.5\ \mu$s) were not possible because of an interfering fluorescence detected through the 308-nm band-pass filter. The fluorescence was observed immediately after the photolysis pulse (without the probe laser) when nitric acid ($\mathrm{HNO_3}$ or $\mathrm{DNO_3}$) was present in the reaction cell. The strength of the fluorescence signal was a nonlinear function of the photolysis laser power, and we attribute the fluorescence to OH($A^2\Sigma^+$) produced by multiphoton photolysis of nitric acid. Fluorescence around 308 nm immediately after 248-nm photolysis of $\mathrm{HNO_3}$ has been previously noted by MacLeod et al.,[12] who also described a very similar fluorescence from pernitric acid (PNA, $\mathrm{HOONO_2}$). In the case of PNA, they attributed the fluorescence to OH($A^2\Sigma^+$) produced by three-photon photolysis of PNA. The OH($A^2\Sigma^+$) fluorescence from photolysis of $\mathrm{HNO_3}$ restricted the temporal profiles to measurements made after 2.5 μs, which limited the precision of the fitted value of k_6'. [Large nitric acid concentrations, needed to maintain adequate OH($v = 1$) signal, led to a 10−60% loss of OH/OD($v = 2$) within 2.5 μs.]

The decay rate coefficient k_2' was measured at various concentrations of $\mathrm{HNO_3}$. A weighted linear least-squares fit of k_2' vs $[\mathrm{HNO_3}]$ yielded the bimolecular rate coefficient k_2. For reaction 3, OH($v = 1$) was monitored with both $\mathrm{HNO_3}$ and $\mathrm{DNO_3}$ present. In this case, OH($v = 2$) was quenched to OH($v = 1$) by both isotopomers, and OH($v = 1$) was lost via reactions with both isotopomers, reactions 2 and 3. The temporal profiles were fit to eq I, with k_2' replaced with $k' = k_2[\mathrm{HNO_3}] + k_3[\mathrm{DNO_3}]$. The concentration of $\mathrm{HNO_3}$ was held constant while that of $\mathrm{DNO_3}$ was varied; the slope of the linear fit of k' vs $[\mathrm{DNO_3}]$ yielded the bimolecular rate coefficient k_3.

The temporal behavior of OD($v = 1$) showed the same biexponential behavior, and the measured temporal profiles of this species were analyzed using the same method as employed for OH($v = 1$) to obtain k_4 and k_5. Figure 3 shows typical plots of pseudo-first-order rate coefficients $k_2'-k_5'$ obtained at ~296 K versus the concentration of $\mathrm{HNO_3}$ or $\mathrm{DNO_3}$.

The ratio of the fitted values of k_6' and k_2' was used to estimate the rate coefficient k_6 ($\equiv k_{6a} + k_{6b}$) relative to k_2; similar ratios of the first-order rate coefficients for the rise and loss of OH/OD($v = 1$) were used to estimate the rate coefficients for reactions 7−9

$$\mathrm{OH}(v=2) + \mathrm{DNO_3} \rightarrow \text{loss of OH}(v=2) \quad (7)$$

$$\mathrm{OD}(v=2) + \mathrm{HNO_3} \rightarrow \text{loss of OD}(v=2) \quad (8)$$

$$\mathrm{OD}(v=2) + \mathrm{DNO_3} \rightarrow \text{loss of OD}(v=2) \quad (9)$$

As noted above, the precision of the fitted value for the rate coefficient for the rise of OH/OD($v = 1$) was quite poor, so only rough estimates of the rate coefficients k_6-k_9 were possible.

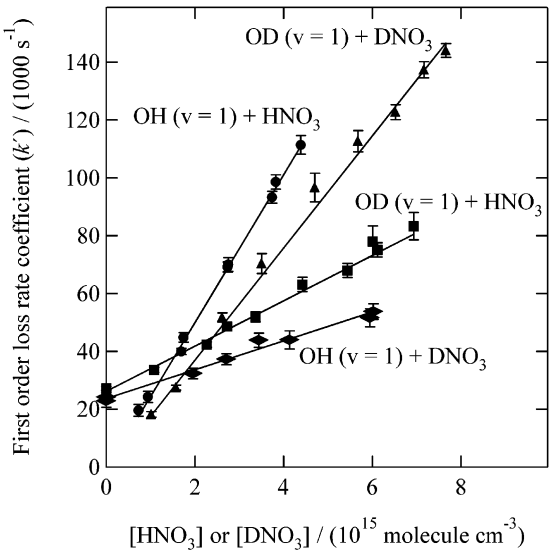

Figure 3. Pseudo-first-order rate coefficients $k_2'-k_5'$ versus the concentration of HNO_3 or DNO_3 at ~296 K. Circles, k_2'; diamonds, k_3'; squares, k_4'; triangles, k_5'. The slopes of these plots are the second-order rate coefficients k_2-k_5: $k_2 = (2.55 \pm 0.12) \times 10^{-11}$, $k_3 = (5.0 \pm 0.5) \times 10^{-12}$, $k_4 = (7.8 \pm 0.5) \times 10^{-12}$, $k_5 = (1.94 \pm 0.07) \times 10^{-11}$ (all in units of cm^3 $molecule^{-1}$ s^{-1}). The large intercepts for k_3 and k_4 are due to the removal of OH($v = 1$) or OD($v = 1$) by HNO_3 or DNO_3, respectively (i.e., due to the reaction of the vibrationally excited radical with its photolytic precursor).

Anhydrous HNO_3 and DNO_3 were prepared by vacuum distillation of the nitric acid formed by the addition of H_2SO_4 or D_2SO_4 to $NaNO_3$. HNO_3 and DNO_3 concentrations were measured by absorption, at room temperature, using the 213.9-nm line from a Zn lamp and 100-cm absorption cells immediately upstream of the LIF reactor [$\sigma_{213.9\ nm}(HNO_3) = (4.52 \pm 0.19) \times 10^{-19}$ cm^2].[1] The absorption cross section of DNO_3 at this wavelength was obtained by measuring the absorption as a function of the pressure of DNO_3 and was found to be 4.5×10^{-19} cm^2. The nitric acid/He mixture flowed through only glass tubing and Teflon fittings before the reaction cell to prevent the decomposition of nitric acid on surfaces such as stainless steel.

Results and Discussion

Yields of OH($v = 1$) and OH($v = 2$) from 248-nm Photolysis of HNO_3. The ratio of the LIF signals of OH($v = 0$) and OH($v = 1$) (back-extrapolated to time zero), normalized by the ratios of the transition probabilities[13] and the laser fluences, gives the ratio of the yield of OH($v = 1$) to that of OH($v = 0$). The ratio is ~1%. The only reported yield of OH ($v = 1$), relative to OH ($v = 0$), from photolysis of HNO_3 at 248 nm is an upper limit of 5%,[14] while the relative yield at 241 nm has been reported to be 2%,[15] in fair agreement with our rough measurement. The quantum yield for OH production from nitric acid photolysis at 248 nm is 1, or close to 1,[16] so the absolute quantum yield for OH($v = 1$) is about 1%. The OH($v = 1$) LIF signal was a linear function of the photolysis laser power, suggesting that multiple-photon processes were not significant. Although we did not measure the yield of OD($v = 1$) from photolysis of DNO_3, the signal levels for OD($v = 1$) were comparable to those for OH($v = 1$) under similar conditions, suggesting that the yield of OD($v = 1$) from 248-nm photolysis of DNO_3 is similar to that of OH($v = 1$) from HNO_3.

To estimate the quantum yield of OH($v = 2$) relative to that of OH($v = 1$), we compared the LIF signals of the two species obtained by probing the $Q_1(1)$ lines of the $A^2\Sigma^+(v' = 0) \leftarrow X^2\Pi(v'' = 1)$ ($\lambda_{air} = 345.85$ nm) and $A^2\Sigma^+(v' = 1) \leftarrow X^2\Pi(v'' = 2)$ ($\lambda_{air} = 350.90$ nm) OH bands. The ratio of the LIF signals was normalized by the transition probabilities for the two excitation lines[13] and the laser powers. To account for the different vibrational states of OH($A^2\Sigma^+$) accessed by the two excitation wavelengths, we corrected the signals by assuming that fluorescence from OH($A^2\Sigma^+$, $v = 0$) occurs in the $Q_1(1)$ line of the $A^2\Sigma^+(v' = 0) \rightarrow X^2\Pi(v'' = 0)$ ($\lambda_{air} = 307.84$ nm)[10] band and that fluorescence from OH($A^2\Sigma^+$, $v = 1$) occurs in the corresponding line of the $A^2\Sigma^+(v' = 1) \rightarrow X^2\Pi(v'' = 1)$ ($\lambda_{air} = 313.46$ nm) band.[10] Therefore, the LIF signals were further normalized by the transition probabilities of these transitions and by the transmission of the band-pass filter on the PMT at these two wavelengths. The resulting quantum yield of OH($v = 2$) is roughly 30% of that of OH($v = 1$), i.e., an absolute quantum yield of roughly 0.003.

The yield of OH($v = 2$), relative to that of OH($v = 1$), was estimated a second way by comparing the fitted values of the initial concentrations, $[OH(v = 2)]_0$ and $[OH(v = 1)]_0$, from the temporal profiles (eq I). Assuming that $k_6 = k_{6a}$, comparison of the fitted values indicates that the yield of OH($v = 2$) from 248-nm photolysis of nitric acid is approximately 40% of that of OH($v = 1$), i.e., a quantum yield of 0.004. However, because k_6 might well be greater than k_{6a}, this ratio of yields is actually a lower limit. Given that estimates of the OH($v = 2$) yield from the fits of the temporal profiles and the comparison of LIF signals are both rather imprecise, the agreement is good. The agreement in the relative yields of OH($v = 2$) estimated by these two methods suggests that k_6 is indeed approximately equal to k_{6a}, i.e., that OH($v = 2$) only loses one quantum of vibrational energy to nitric acid per "reaction".

The relative quantum yields of the vibrational states of OH from 248-nm photolysis are somewhat surprising: Only about 1% of the OH is vibrationally excited, and the yield of OH($v = 2$) is ~30−40% of that of OH($v = 1$). This might be due to efficient multiphoton photolysis of HNO_3,[15,17] although the ratio $[OH(v = 1)]_0/[OH(v = 2)]_0$, as calculated from the fits to eq I, did not vary with the photolysis laser power as the fluence was varied from 2.7 to 21 mJ/cm^2. The ratio also did not vary significantly when N_2 (~2 Torr), which efficiently quenches $O(^1D)$, was added to the reaction mixture, suggesting that $O(^1D)$ (conceivably formed in the photolysis of HNO_3) is not an important precursor of vibrationally excited OH. The directly observed single-exponential temporal profile of OH($v = 2$) suggests that, if OH($v > 2$) is produced by HNO_3 photolysis at this wavelength, it is produced only in small amounts relative to OH($v = 2$).

Rate Coefficients k_2-k_5. The rate coefficients for removal of OH($v = 1$) and OD($v = 1$) by HNO_3 and DNO_3 and the temperature dependence of these rate coefficients are reported in Table 1 and displayed in Figure 4. The figure also shows the previously reported values of k_2 and k_5 at room temperature;[7] the agreement between the previously reported measurements and values obtained in the present work is excellent. All of these rate coefficients are much larger (by a factor of 50−1200) than the rate coefficients for the *reactions* of OH($v = 0$) and OD($v = 0$) with HNO_3 and DNO_3 under similar experimental conditions.[1,2] It is unlikely that this difference in rate coefficients for removal of the vibrationally excited and vibrationally unexcited radicals can be explained by an increase in the *reaction* rate coefficients due to the vibrational excitation of the OH or OD radical. Therefore, the primary removal process for OH/OD($v = 1$) is likely *relaxation* of the vibrationally

TABLE 1: Measured Rate Coefficients for the Loss of OH($v = 1$) or OD($v = 1$) by HNO_3 and DNO_3

reaction	temperature (K)	$[HNO_3]$ or $[DNO_3]^{a,b}$	$k \pm 2\sigma^{c,d}$
OH($v = 1$) + HNO_3 (k_2)	252.3	4.5−30.7	31.3 ± 1.5
	271.0	5.3−31.1	26.1 ± 1.6
	295.3	7.3−43.9	25.5 ± 1.2
	295.5	3.5−32.4	24.5 ± 1.3
	330.9	4.2−25.0	17.6 ± 1.3
	373.1	2.3−18.5	15.8 ± 1.5
OH($v = 1$) + DNO_3 (k_3)	253.0	8.6−51.7	9.1 ± 0.4
	276.5	5.8−40.8	6.9 ± 0.5
	295.6	4.9−32.3	6.5 ± 0.5
	295.7	19.5−60.2	5.0 ± 0.5
	333.7	4.7−39.9	4.4 ± 0.4
	363.0	6.1−33.3	3.8 ± 0.4
OD($v = 1$) + HNO_3 (k_4)	252.7	22.7−118.7	11.4 ± 0.5
	259.8	8.9−59.1	10.5 ± 0.5
	295.0	16.4−74.9	8.4 ± 0.7
	295.0	11.6−101.1	7.9 ± 0.3
	295.2	10.6−53.3	8.3 ± 0.5
	295.2	11.7−85.4	8.1 ± 0.5
	296.0	10.8−69.3	7.8 ± 0.5
	373.7	9.0−58.8	3.5 ± 0.5
	383.9	16.5−100.9	4.75 ± 0.17
OD($v = 1$) + DNO_3 (k_5)	259.8	10.8−45.7	25.1 ± 1.1
	259.8	9.9−82.5	24.6 ± 0.8
	295.2	7.1−39.7	15.3 ± 1.0
	295.2	8.0−77.7	18.0 ± 0.6
	295.2	10.2−76.6	19.4 ± 0.7
	373.1	4.9−52.6	12.2 ± 0.4

[a] Concentration of reactant in excess. [b] Units are 10^{14} cm^{-3}. [c] Units are 10^{-12} cm^3 molecule^{-1} s^{-1}. [d] Reported uncertainties are statistical only.

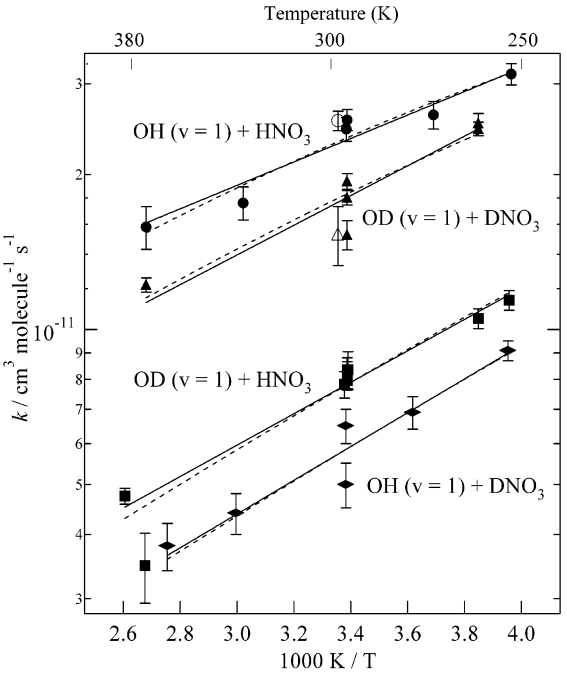

Figure 4. Arrhenius representation of k_2-k_5. Filled symbols, this work; open symbols, ref 7. Circles, k_2; diamonds, k_3; squares, k_4; triangles, k_5. The solid lines are Arrhenius fits (see Table 2 for fit parameters), and the dashed lines are fits to expression III (see text). The error bars are statistical only (2σ), representing the uncertainty from the fit of k' vs $[HNO_3]$ or $[DNO_3]$.

excited radicals by HNO_3 and DNO_3. We also note that the arguments presented below do not rely upon any assumption about whether OH/OD($v = 1$) is lost by reaction with HNO_3/DNO_3 or is relaxed by HNO_3/DNO_3 to OH/OD($v = 0$).

TABLE 2: Parameters for Fits of k_2-k_5 to Arrhenius Expression and Expression II[a]

	$k(T) = Ae^{-E_a/RT}$		$k(T) = k(298)(T/298)^{-n}$	
reaction	A^b	E_a/R (K)	$k(298)^c$	n
OH($v = 1$) + HNO_3	40 ± 20	−520 ± 140	23.2 ± 1.3	1.8 ± 0.5
OH($v = 1$) + DNO_3	4.7 ± 3.4	−750 ± 200	5.8 ± 0.5	2.6 ± 0.8
OD($v = 1$) + HNO_3	7.2 ± 3.5	−700 ± 140	7.8 ± 0.4	2.4 ± 0.4
OD($v = 1$) + DNO_3	19 ± 15	−660 ± 220	17.9 ± 1.6	2.2 ± 0.8

[a] Error bars are 2σ representations of the uncertainty of the fits. [b] Units are 10^{-13} cm^3 molecule^{-1} s^{-1}. [c] Units are 10^{-12} cm^3 molecule^{-1} s^{-1}.

The rate coefficients for the removal of OH/OD($v = 2$) by HNO_3/DNO_3, k_6-k_9, are roughly 3−6 times larger than the corresponding rate coefficients k_2-k_5. This ratio is roughly the same for each isotopic combination. However, the ratio did increase somewhat with increasing temperature, so the rate coefficients k_6-k_9 appear to show a weaker negative temperature dependence (see below) than the rate coefficients k_2-k_5.

Any proposed mechanism for these processes must explain three aspects of the measured rate coefficients. First, all of the rate coefficients correspond to quite facile loss of OH/OD($v = 1$). Thus, comparing the rate coefficients in Table 1 with simple estimates of the rate coefficients for collisions between OH/OD and HNO_3/DNO_3 on a simple hard-sphere, or hard-sphere with Lennard-Jones attraction, basis leads to collisional probabilities for loss of OH/OD($v = 1$) of between 0.1 and 0.01. Second, we note that all of the rate coefficients show a quite steep *negative* dependence on temperature and that they vary with temperature in a very similar fashion. Table 2 lists the parameters for nonlinear least-squares fits (unweighted) of the rate coefficients k_2-k_5 to two temperature-dependence formalisms, the Arrhenius expression and the expression

$$k(T) = k(298)(T/298)^{-n} \qquad \text{(II)}$$

The Arrhenius fits are also shown in Figure 4. Thus, expressed as negative activation energies, the temperature dependences yield values of E_a/R varying from −(520 ± 140) K for reaction 2 to −(750 ± 200) K for reaction 3. If, instead, the rate coefficients are fit to expression II, then n varies from (1.8 ± 0.5) for reaction 2 to (2.6 ± 0.8) for reaction 3. The negative activation energies and n are not physically meaningful, but rather are empirical quantities to describe the negative temperature dependence of these reactions, within the temperature range of these experiments. Finally, any proposed mechanism should explain the differences between the absolute magnitudes of the rate coefficients, particularly the fact that those for the fully hydrogenated and fully deuterated isotopic pairs (reactions 2 and 5) are greater than those for the mixed isotopic pairs (reactions 3 and 4).

One possible explanation for the larger values of k_2 and k_5 compared to k_3 and k_4 is that at least some fraction of the OH/OD($v = 1$) loss occurs via near-resonant *inter*molecular vibration−vibration (V−V) energy transfer. Such processes can be written as

$$\text{OH}(v = 1) + \text{HNO}_3 \rightarrow \text{OH}(v = 0) + \text{HNO}_3(\nu_1), \quad (\Delta E/hc) = -20 \text{ cm}^{-1} \qquad (10)$$

$$\text{OD}(v = 1) + \text{DNO}_3 \rightarrow \text{OD}(v = 0) + \text{DNO}_3(\nu_1), \quad (\Delta E/hc) = -11 \text{ cm}^{-1} \qquad (11)$$

where $HNO_3(\nu_1)$ and $DNO_3(\nu_1)$ denote molecules with one quantum of vibrational excitation in the OH/OD stretching mode

of the molecule. In view of the close resonance between the vibrational transition energies in the collision partners in these processes, intermolecular V−V energy transfer might contribute to the loss rate coefficients in the cases of $OH(v = 1) + HNO_3$ and $OD(v = 1) + DNO_3$. However, in the mixed isotopic pairs, such V−V exchange processes

$$OD(v = 1) + HNO_3 \rightarrow OD(v = 0) + HNO_3(\nu_1), \quad (\Delta E/hc) = +908\ cm^{-1} \quad (12)$$

$$OH(v = 1) + DNO_3 \rightarrow OH(v = 0) + DNO_3(\nu_1), \quad (\Delta E/hc) = -940\ cm^{-1} \quad (13)$$

are nonresonant, and reaction 12 is also strongly endothermic. (Acceptance of the vibrational energy by other modes of HNO_3 would not be endothermic, but it would be nonresonant.) Clearly, intermolecular V−V energy transfer will not be efficient for reactions 3 and 4. Yet, the rate coefficients k_3 and k_4 are still quite large: for example, the room-temperature rate coefficients for the removal of $OH(v = 1)$ by CH_4 and CO_2 are about 10 and 20 times smaller, respectively.[18]

These observations can be explained if the loss of $OH/OD(v = 1)$ in the presence of HNO_3/DNO_3 occurs via formation of the hydrogen-bonded complex that has been invoked to explain the unusual kinetic behavior of the chemical reaction between OH radicals and HNO_3.[2] This mechanism can be discussed in terms of the following scheme of elementary processes, here written for $OH(v = 1) + HNO_3$

$$OH\ (v = 1) + HNO_3 \underset{k_{-a}}{\overset{k_a}{\rightleftharpoons}} OH(v = 1)\cdot HNO_3^{*} \xrightarrow{k_{IVR}} OH\ (v = 0) + HNO_3 \xleftarrow{k_{-b}} OH(v = 0)\cdot HNO_3^{**}$$

Here, $OH(v = 1)\cdot HNO_3^*$ signifies a hydrogen-bonded complex formed in collisions of $OH(v = 1)$ with HNO_3 in which the energy originally in the vibration of the OH radical remains localized in this vibration in the complex. The rate coefficients k_a and k_{-a} are those associated with the bimolecular formation of this complex and its unimolecular dissociation, respectively. k_{IVR} is the rate coefficient for intramolecular vibrational redistribution (IVR) of the energy from the OH radical vibration in $OH(v = 1)\cdot HNO_3^*$ to the other modes of the complex, yielding $OH(v = 0)\cdot HNO_3^{**}$, in which the radical OH stretch is unexcited, but which contains more energy in its other vibrational modes. Given the far higher density of states associated with the low mode frequencies, it is fair to assume that the reverse transfer is unimportant within the lifetime of the $OH(v = 0)\cdot HNO_3^{**}$ complex. This complex will dissociate rapidly (i.e., $k_{-b} > k_{-a}$) on account of its high content of internal energy relative to ground-state $OH(v = 0) + HNO_3$. Of course, the complexes $OH(v = 1)\cdot HNO_3^*$ and $OH(v = 0)\cdot HNO_3^{**}$ might also dissociate to form the products of reaction 1, H_2O and NO_3 (not shown in above scheme). In fact, the rate coefficient for dissociation to H_2O and NO_3 of $OH(v = 0)\cdot HNO_3^{**}$ will likely be significantly larger than the rate coefficient for dissociation to H_2O and NO_3 of $OH(v = 0)\cdot HNO_3^*$, the complex formed by the association of $OH(v = 0)$ and HNO_3, because of the additional energy of the $OH(v = 0)\cdot HNO_3^{**}$ complex. This additional energy is greater than the calculated height[4] of the barrier between $OH(v = 0)\cdot HNO_3^*$ and $H_2O + NO_3$.

According to this mechanism, if the concentration of $OH(v = 1)\cdot HNO_3^*$ is in steady state, the rate coefficient for the loss of $OH(v = 1)$ by HNO_3 will be given by

$$k_X = k_a[k_{IVR}/(k_{IVR} + k_{-a})] \quad (III)$$

We can recognize two limiting cases: (i) when $k_{IVR} \gg k_{-a}$ and $k_X = k_a$ and (ii) when $k_{IVR} \ll k_{-a}$ and $k_X = k_a[k_{IVR}/k_{-a}]$. When strong covalent bonds are made to form a complex, as, for example, in $OH(v = 1) + NO_2$,[6] the first limit is almost certainly reached. In this case, association to form the complex is the rate-determining step. The rate coefficient for loss of the vibrationally excited radical then provides a good estimate of the rate coefficient for association of the two species (usually free radicals) in the limit of high pressure, and we would expect little or no temperature dependence of the rate coefficient for the loss of the vibrationally excited radical. For example, the rate coefficients for the removal of $CH(v = 1)$ by H_2 or D_2[19] and for the removal of $OH(v = 1)$ by SO_2[20] show small negative temperature dependences: when they are fit to expression II, *n*, the absolute value of the exponent, is at most 0.27. If this limit is reached in the present systems, we would also expect the rate coefficients for the loss of $OH/OD(v = 1)$ to be similar for all isotopic pairs that we have studied, as observed for the loss of $CH(v = 1)$ by H_2 and D_2.[19]

In the second limit, k_X will be much less than k_a. Moreover, the expression for k_X is similar to that for recombination in the limit of low pressure, with k_{IVR} replacing the rate coefficient for collisions that remove energy from the addition complex. Generally, such rate coefficients show a steep, *negative* temperature dependence that can be viewed in one of two ways: either one can show, via statistical mechanics, that the ratio k_a/k_{-a} decreases with increasing temperature, or equivalently, one can show that k_{-a} increases more steeply with temperature than either k_a or the frequency of deactivating collisions. In the present cases, we do not believe that either limit (i) ($k_{IVR} \gg k_{-a}$) or limit (ii) ($k_{IVR} \ll k_{-a}$) applies. The temperature dependence of the rate coefficients, which gets somewhat steeper as the rate coefficients decrease, depends largely on the increase in k_{-a} as the temperature is increased. We note that, even for $OH(v = 1) + HNO_3$, which has the largest value of k_X, the rate coefficients have an appreciable negative dependence on temperature, strongly suggesting that, in all cases we have studied, $k_X < k_a$ and IVR is not very fast compared to the dissociation of $OH(v = 1)\cdot HNO_3^*$. Given the structure of the $OH\cdot HNO_3$ complex presented in ab initio studies[4,5] (see Figure 1), it seems plausible that IVR is relatively slow from the radical OH stretch into the other modes of the complex, as the OH is only loosely bound (<8 kcal) at some distance (~2 Å) from the HNO_3 molecule in the complex.

Herbert et al.[21] observed that the removal of $CH(v = 1)$ by N_2 is rapid [$k(294\ K) = 3.0 \times 10^{-11}\ cm^3\ molecule^{-1}\ s^{-1}$] and that the rate coefficient for this process shows a moderate negative temperature dependence between 86 and 584 K: when fit to expression II, *n* was ~1.2. They attribute the fast removal of $CH(v = 1)$ by N_2 to the formation of the weakly-bound CHN_2 species: the strength of the dative bond between CH and N_2 is approximately 30 kcal mol^{-1}.[22] Herbert et al. suggest that the CHN_2 complex might dissociate before the CH vibrational excitation energy is redistributed to the other modes of the complex. Thus, the rate coefficient shows a negative temperature dependence. Furthermore, high-pressure measurements[23] of the rate coefficients for the reaction of ground-state CH with N_2 from 200 to 500 K show that the high-pressure limit for this rate coefficient is nearly temperature-independent ($n = 0.15$) and it is slightly higher than the rate coefficients for loss of $CH(v = 1)$ by N_2. In the case of $OH(v = 1) + HNO_3$, the bond

formed between the two species is weaker still, and the rate coefficients show a stronger negative temperature dependence.

Finally, we address the question of why the magnitude of the rate coefficients for loss of OH/OD($v = 1$) in the different isotopic systems differ, with those for the like-isotope combinations (k_2 and k_5) being larger than those for the unlike-isotope combinations (k_3 and k_4). We believe that the most likely explanation for this lies in the different rates of *intra*molecular vibrational relaxation in the different systems. The fully hydrogenated and fully deuterated systems offer a route for IVR that is not available in the mixed systems, namely, V−V transfer, *within the complex*, from the vibration associated with the radical to the OH/OD stretch in HNO_3/DNO_3. This pathway is nonresonant in the isotopically mixed complexes. Subsequent transfer into the low-frequency modes, i.e., those within the HNO_3 or DNO_3 moiety or the intermolecular modes of the complex, is likely to be more efficient from these modes that are strongly coupled to the low-frequency modes than directly from the vibration of the OH/OD radical.

Intermolecular V−V energy transfer is probably not a major contributor to any of the rate coefficients k_2-k_5. For the unlike-isotope processes, reactions 3 and 4, the lack of resonance between the collision partners means that intermolecular energy transfer will be inefficient: rate coefficients similar to those for the quenching of OH($v = 1$) by CH_4 and CO_2[18] would be expected if the removal of OH/OD($v = 1$) occurred via intermolecular energy transfer. The like-isotope processes are faster, but the negative temperature dependences are quite similar for the like- and unlike-isotope processes. Therefore, the process that occurs in the like-isotope systems but not in the unlike-isotope systems also has a strong negative temperature dependence. Intermolecular V−V energy transfer should be weakly temperature-dependent, and thus, it is unlikely to account for the differences between the rate coefficients for the like- and unlike-isotope processes. Therefore, the larger rate coefficients for the like-isotope processes are probably due to faster V−V transfer within the hydrogen-bonded complex.

To test the validity of expression III, we fitted the rate coefficients k_2-k_5 to this expression. Figure 4 shows, as dashed lines, the results of the global fit. k_a and k_{-a} were assumed to be the same for reactions 2−5; only k_{IVR} was allowed to vary between reactions. Furthermore, k_a and k_{IVR} were assumed to be temperature-independent, whereas k_{-a} was assumed to have an Arrhenius temperature dependence

$$k_{-a} = A \exp(-E_a/RT) \qquad \text{(IV)}$$

The fitted value of k_a is $(7 \pm 5) \times 10^{-11}$ cm^3 molecule^{-1} s^{-1}, indicating that the OH·HNO_3* complex is formed efficiently from the free reactants. (Quoted errors represent the uncertainty of the nonlinear least-squares fit, at the 2σ level.) The "activation energy" for dissociation of the complex, E_a/R, is 840 ± 280 K. The remaining parameters, k_{IVR} and A, the preexponential factor of k_{-a}, are not independent variables in expression III, so they cannot be assigned by the fit. However, k_{-a}, like k_a, should be unaffected by the vibrational excitation of the OH radical: it should be the same for OH($v = 1$)·HNO_3* and OH($v = 0$)·HNO_3*, the complex formed by the association of OH($v = 0$) and HNO_3, because the extra energy in the OH($v = 1$)·HNO_3* complex is localized in the radical OH stretch and does not affect other modes of the complex. As described previously,[2] the ratio k_a/k_{-a} is roughly constrained by the thermodynamics of the OH·HNO_3 complex, which allows us to assign an approximate value for A of 3×10^{12} s^{-1}. The resulting values of k_{IVR} for the four different reactions from the constrained fit are given in Table 3. Because these values of k_{IVR} depend on the estimated value of A, their absolute magnitude is not as significant as their values relative to one another. However, these values correspond to reasonable lifetimes with respect to IVR (10−60 ps). For example, Wheeler et al.[24] reported that the OH($v = 1$) complex with CH_4 has a lifetime of 38 ± 5 ps. The fact that we are able to fit k_2-k_5 to expression III using reasonable values for the elementary rate coefficients demonstrates that our data are consistent with the mechanism we present for the removal of OH($v = 1$) and OD($v = 1$) by HNO_3 and DNO_3. The mechanism not only accounts for the different magnitude of the rate coefficients k_2-k_5 and their temperature dependence, but also accounts for the slight increase in the strength of the negative temperature dependence in the slower reactions.

TABLE 3: Values of k_{IVR} from the Fit of k_2-k_5 to Expression III[a]

reaction	$(k_{IVR} \pm 2\sigma)/10^{10}$ s^{-1}
OH($v = 1$) + HNO_3	9.2 ± 4.4
OH($v = 1$) + DNO_3	1.7 ± 0.7
OD($v = 1$) + HNO_3	2.3 ± 0.9
OD($v = 1$) + DNO_3	6.4 ± 2.8

[a] Error bars represent the uncertainty of the fits.

Furthermore, the rate coefficients we report here are consistent with the observed pressure- and temperature-dependent kinetics for the reaction of OH($v = 0$) with HNO_3. Previous work from our laboratory[2] has simulated the pressure- and temperature-dependent rate coefficient for this reaction, k_1, using the mechanism shown in Figure 1. k_a was estimated to be 1×10^{-11} cm^3 molecule^{-1} s^{-1}. This estimate was based on the previous measurements of k_2 and k_5 by Smith and Williams,[7] with the assumption that some loss of OH($v = 1$) occurs by resonant V−V transfer without formation of the OH·HNO_3 complex. Here, we argue that resonant V−V transfer without complex formation is unimportant and that k_a is probably larger than the rate coefficients presented here and previously for reactions 2−5: the fit of our data to expression III gives $k_a = 7 \times 10^{-11}$ cm^3 molecule^{-1} s^{-1}. Our fit to expression III also provides the temperature dependence of k_{-a}. Using this updated information about the elementary rate coefficients for the mechanism shown in Figure 1, k_1 can be simulated as described previously, with only minor adjustments to the previously presented rate coefficients for the various steps of the reaction.

We conclude that the loss of vibrationally excited OH($v = 1$) and OD($v = 1$) in the systems that we have studied occurs via relaxation by formation of hydrogen-bonded complexes. However, in none of these cases does the rate coefficient for loss of OH/OD($v = 1$) reach that for bimolecular formation of the collision complex (k_a), because the rate coefficients for redissociation of the initially formed complexes (k_{-a}) and for intramolecular vibrational redistribution of the OH/OD excitation energy into the other modes of the complex (k_{IVR}) are similar. We attribute the negative temperature dependence of the values of k_2-k_5 to the increasing rate of redissociation of the complexes as the temperature is increased. Finally, we propose that different rates of intramolecular vibrational energy redistribution might be responsible for the different loss rate coefficients in the four systems that we have studied.

Acknowledgment. This work was funded in part by the NASA Upper Atmospheric Research Program. D.C.M. acknowledges an NSF graduate research fellowship.

References and Notes

(1) Brown, S. S.; Talukdar, R. K.; Ravishankara, A. R. *J. Phys. Chem. A* **1999**, *103*, 3031.
(2) Brown, S. S.; Burkholder, J. B.; Talukdar, R. K.; Ravishankara, A. R. *J. Phys. Chem. A* **2001**, *105*, 1605.
(3) Margitan, J. J.; Watson, R. T. *J. Phys. Chem*. **1982**, *86*, 3819.
(4) Xia, W. S.; Lin, M. C. *J. Chem. Phys.* **2001**, *114*, 4522.
(5) Aloisio, S.; Francisco, J. S. *J. Phys. Chem. A* **1999**, *103*, 6049.
(6) Smith, I. W. M. *J. Chem. Soc., Faraday Trans.* **1997**, *93*, 3741.
(7) Smith, I. W. M.; Williams, M. D. *J. Chem. Soc., Faraday Trans. 2* **1985**, *81*, 1849.
(8) Jaffer, D. H.; Smith, I. W. M. *Faraday Discuss. Chem. Soc*. **1979**, *67*, 212.
(9) Vaghjiani, G. L.; Ravishankara, A. R. *J. Phys. Chem.* **1989**, *93*, 1948.
(10) Dieke, G. H.; Crosswhite, H. M. *J. Quant. Spectrosc. Radiat. Transfer* **1962**, *2*, 97.
(11) Clyne, M. A. A.; Coxon, J. A.; Woon Fat, A. R. *J. Mol. Spectrosc*. **1973**, *46*, 146.
(12) MacLeod, H.; Smith, G. P.; Golden, D. M. *J. Geophys. Res.* **1988**, *93*, 3813.
(13) Luque, J.; Crosley, D. R. *LIFBASE: Database and Simulation Program*, v. 1.6; SRI Report No. MP 99-009; SRI International: Menlo Park, CA, 1999.
(14) Schiffman, A.; Nelson, D. D.; Nesbitt, D. J. *J. Chem. Phys.* **1993**, *98*, 6935.
(15) Sinha, A.; Vander Wal, R. L.; Crim, F. F. *J. Chem. Phys.* **1989**, *91*, 2929.
(16) Sander, S. P.; Friedl, R. R.; Golden, D. M.; Kurylo, M. J.; Huie, R. E.; Orkin, V. L.; Moortgat, G. K.; Ravishankara, A. R.; Kolb, C. E.; Molina, M. J.; Finlayson-Pitts, B. J. *Chemical Kinetics and Photochemical Data for Use in Atmospheric Studies, Evaluation Number 14*; JPL Publication No. 02-25; Jet Propulsion Laboratory: Pasadena, CA, 2003.
(17) Suto, M.; Lee, L. C. *J. Chem. Phys.* **1984**, *81*, 1294.
(18) Raiche, G. A.; Jeffries, J. B.; Rensberger, K. J.; Crosley, D. R. *J. Chem. Phys.* **1990**, *92*, 7258.
(19) Brownsword, R. A.; Canosa, A.; Rowe, B. R.; Sims, I. R.; Smith, I. W. M.; Stewart, D. W. A.; Symonds, A. C.; Travers, D. *J. Chem. Phys.* **1997**, *106*, 7662.
(20) Blitz, M. A.; Hughes, K. J.; Pilling, M. J. *J. Phys. Chem. A* **2003**, *107*, 1971.
(21) Herbert, L. B.; Sims, I. R.; Smith, I. W. M.; Stewart, D. W. A.; Symonds, A. C.; Canosa, A.; Rowe, B. R. *J. Phys. Chem.* **1996**, *100*, 14928.
(22) Moskaleva, L. V.; Lin, M. C. *Z. Phys. Chem.* **2001**, *215*, 1043 and references therein.
(23) Fulle, D.; Hippler, H. *J. Chem. Phys.* **1996**, *105*, 5423.
(24) Wheeler, M. D.; Tsiouris, M.; Lester, M. I.; Lendvay, G. *J. Chem. Phys.* **2000**, *112*, 6590.